Earth and Planetary Science Letters 425 (2015) 179–186

Contents lists available at ScienceDirect

Earth and Planetary Science Letters

www.elsevier.com/locate/epsl

Transtensional deformation of Montserrat revealed by shear wave splitting

Alan F. Baird [a,*], J.-Michael Kendall [a], R. Stephen J. Sparks [a], Brian Baptie [b]

[a] School of Earth Sciences, University of Bristol, Queen's Road, Bristol BS8 1RJ, UK
[b] British Geological Survey, West Mains Road, Edinburgh EH9 3LA, UK

ARTICLE INFO

Article history:
Received 6 January 2015
Received in revised form 30 May 2015
Accepted 2 June 2015
Available online 11 June 2015
Editor: P. Shearer

Keywords:
anisotropy
shear-wave splitting
transtension
Montserrat

ABSTRACT

Here we investigate seismic anisotropy of the upper crust in the vicinity of Soufrière Hills volcano using shear wave splitting (SWS) analysis from volcano-tectonic (VT) events. Soufrière Hills, which is located on the island of Montserrat in the Lesser Antilles, became active in 1995 and has been erupting ever since with five major phases of extrusive activity. We use data recorded on a network of seismometers between 1996 and 2007 partially spanning three extrusive phases. Shear-wave splitting in the crust is often assumed to be controlled either by structural features, or by stress aligned cracks. In such a case the polarization of the fast shear wave (ϕ) would align parallel to the strike of the structure, or to the maximum compressive stress direction. Previous studies analyzing SWS in the region using regional earthquakes observed temporal variations in ϕ which were interpreted as being caused by stress perturbations associated with pressurization of a dyke. Our analysis, which uses much shallower sources and thus only samples the anisotropy of the upper few kilometres of the crust, shows no clear temporal variation. However, temporal effects cannot be ruled out, as large fluctuations in the rate of VT events over the course of the study period as well as changes in the seismic network configuration make it difficult to assess. Average delay times of approximately 0.2 s, similar in magnitude to those reported for much deeper slab events, suggest that the bulk of the anisotropy is in the shallow crust. We observe clear spatial variations in anisotropy which we believe are consistent with structurally controlled anisotropy resulting from a left-lateral transtensional array of faults which crosses the volcanic complex.

1. Introduction

Active volcanoes experience dynamic processes such as dyke pressurization, and the migration of magmatic, hydrothermal and meteoric fluids, which may produce complex heterogeneous stress fields. This may be further complicated through their interaction with local tectonic structures such as active faults. One approach to explore these relationships is through the use of S-wave splitting (SWS) analysis to estimate seismic anisotropy of the crust (e.g. Boness and Zoback, 2006; Johnson et al., 2011). This approach may be used to investigate spatial and temporal changes in rock properties, providing a powerful tool for monitoring volcanoes. Here we investigate seismic anisotropy of the upper crust in the vicinity of Soufrière Hills Volcano (SHV) on the island of Montserrat, using SWS analysis from volcano-tectonic (VT) events.

SWS occurs when S-wave energy propagates through an anisotropic medium as two orthogonally polarized waves that travel at different speeds. A measure of the anisotropy along a ray-path can be characterized by the delay time between the fast and slow wave arrivals (δt) and the polarization direction of the fast wave (ϕ), which provides an indication of the orientation or symmetry of the anisotropy. Anisotropy is typically related either to fabrics associated with geologic structure (e.g. crystal lattice preferred orientation, aligned faults and fractures, sedimentary layering, rock foliation), or to the stress field due to the presence of stress aligned microcracks. Therefore, temporal variations in anisotropy can be interpreted in terms of changes in the stress field (e.g. Teanby et al., 2004a).

There have been growing number of studies using SWS to investigate anisotropy in volcanic settings, many of which link observations of temporal changes in anisotropy to stress changes associated with volcanological processes (e.g. Gerst and Savage, 2004; Keats et al., 2011; Johnson and Savage, 2012). Care must be taken, however, to determine whether the observed SWS is related to stresses (i.e. through stress-aligned microcracks) or to structural anisotropy (Boness and Zoback, 2006; Johnson et al., 2011). Similar effects have been observed in petroleum reservoirs (e.g. Teanby et al., 2004a; Baird et al., 2013).

* Corresponding author.
E-mail address: alan.baird@bristol.ac.uk (A.F. Baird).

http://dx.doi.org/10.1016/j.epsl.2015.06.006

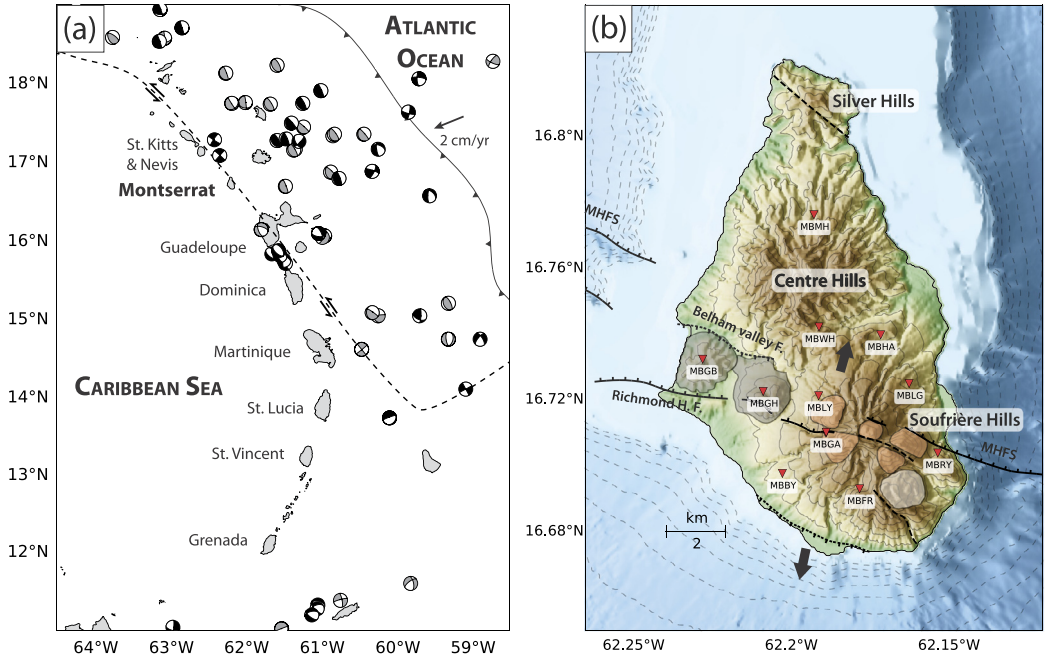

Fig. 1. (a) Location of Montserrat within the Lesser Antilles arc showing focal mechanisms from shallow earthquakes (black <20 km and grey <40 km depth) from the Global CMT Project catalog. Dashed line indicates the proposed strike-slip boundary of the northern Lesser Antilles forearc block (López et al., 2006). (b) Map of Montserrat showing the location of the stations used in the study, active faults (solid black lines), less active or inferred faults (black dashed lines), and volcanic complexes coloured by age. In orange are the Soufrière Hills domes (170 ka to present), in white is the South Soufrière Hills dome, and in grey Garibaldi Hill and St. Georges Hill (~282 ka). Light grey lines indicate topographic contours, and double black arrows indicate local direction of extension (after Feuillet et al., 2010). (For interpretation of the references to color in this figure legend, the reader is referred to the web version of this article.)

Previous work investigating SWS on Montserrat (Roman et al., 2011) used regional earthquakes. These regional earthquakes were not associated with volcanological processes on Montserrat but related to the tectonics of the Lesser Antilles region. They found that at most stations ϕ was oriented primarily NE–SW, but temporal variations in ϕ were observed in the months preceding the onset of extrusive activity at SHV in 1999. This temporal variation was found to be coincident with an observed change in the p-axis orientation of volcano tectonic earthquakes from dominantly NE–SW to NW–SE (Roman et al., 2006, 2008). Together, these observations were interpreted as being caused by the pressurization of a NE–SW oriented dyke prior to the eruption, which temporarily perturbed the surrounding stress field. Others, however, disagree with the NE–SW dyke interpretation (e.g. Hautmann et al., 2009).

A major drawback of the approach of Roman et al. (2011) is that ray-paths from regional earthquakes may pass through very different geological environments, possibly with different anisotropic fabrics, before arriving at the station. It is therefore difficult to constrain where along the ray-path the observed SWS has accrued. Nevertheless, Roman et al. (2011) interpreted their observations under the assumption that most of the SWS occurred in the crust beneath the island. In this paper we investigate SWS using local volcano-tectonic earthquakes as sources. In doing so we ensure that any observed anisotropy is localized in the upper few kilometres of the crust. We consider seismicity recorded between 1996 and 2007, partially spanning three extrusive phases.

2. Background

The island of Montserrat lies between the islands of Guadeloupe and Nevis in the Lesser Antilles arc, which was formed as a result of subduction of the North American plate beneath the Caribbean plate. Fig. 1 shows focal mechanisms of shallow earthquakes in the Lesser Antilles. Most of the activity to the east of Montserrat shows thrust mechanisms with p-axes consistent with an arc-normal direction of maximum horizontal compressive stress (S_H). However, it is likely that the upper plate has local tectonic domains where S_H departs markedly from the plate scale system. Wadge (1986) mapped dyke orientations throughout the Lesser Antilles and found evidence of a change in S_H from approximately arc-normal in the northern portion of the arc to arc-parallel in the south, with Montserrat lying near the transition between these two zones. Notably, however, that study did not include dyke observations from Montserrat. Mapping of fault systems in the upper plate in the region around Montserrat (Feuillet et al., 2002, 2010; Kenedi et al., 2010) indicates localized tectonic domains.

More recently, López et al. (2006) found that although the convergence vector between the Caribbean and North American plates is oriented ENE, GPS measurements in the Northern Lesser Antilles suggest the upper plate arc crust is moving in a more northerly direction than expected. They proposed that there is a northern Lesser Antilles forearc block, that is separated from the Caribbean plate by a strike slip fault system accommodating the left lateral component of oblique convergence across the arc. López et al. (2006) proposed a boundary of the block, based on the alignment of shallow strike slip earthquake focal mechanisms, which passes across Montserrat (Fig. 1a, dashed line), suggesting an approximately WNW S_H orientation.

The geology of the island of Montserrat is dominated almost entirely by volcanic rocks in three distinct andesitic volcanic massifs (Le Friant et al., 2004), the oldest being Silver Hills in the North (2600–1200 ka), to the south of which lies the Centre Hills (950–550 ka), and the currently active South Soufrière Hills–Soufrière Hills (170 ka to present) (Fig. 1b). There are a series of WNW trending faults which cross the SHV volcanic complex, the most prominent being the Belham Valley and Richmond Hill faults at the southern portion of the island which extend offshore to the NW forming the Montserrat–Havers fault zone (Feuillet et al., 2010). These faults represent a right-step in an *en echelon* transtensional array of faults accommodating both normal and left-lateral slip, that trend NNW between Montserrat and

Guadeloupe (Feuillet et al., 2002, 2010; Kenedi et al., 2010), representing the boundary of the block proposed by López et al. (2006). Volcanic domes of the most recent Soufrière Hills complex align along a trend coincident with the strike of these faults suggesting that they both formed as a consequence of NNE–SSW crustal extension. This trend, together with the feeder dyke orientation suggested by geophysical data (Hautmann et al., 2009; Linde et al., 2010), indicates an approximately WNW S_H in the vicinity of Montserrat.

2.1. Current eruption and seismicity

As of 2014 the current eruption of Soufrière Hills has comprised five phases of extrusive activity separated by periods of residual activity. Our study, however, only covers the initial three phases of the eruption, the first of which began in late 1995 following three years of increased volcano-tectonic (VT) activity and continued until March 1998. After a pause for approximately 20 months the second phase began in November 1999 and lasted until July 2003 with two short intervals of no extrusion. Two years later the third phase began in August 2005 lasting until April 2007. Two very short extrusion events between July 2008 and January 2009 mark the fourth phase. The most recent phase began in October 2009 and lasted until February 2010. For a more detailed description of the eruption sequence see Wadge et al. (2014).

Seismicity during the eruption was recorded on the Montserrat Volcano Observatory (MVO) digitally telemetered seismic network that was installed by the British Geological Survey in October 1996 to replace an older analogue network (Luckett et al., 2007; Luckett, 2009). This network initially consisted of five three-component broadband sensors and threes vertical sensors; however in 1997 several of these stations were destroyed by pyroclastic flows, and it wasn't until after the first eruptive phase was complete before new stations could be installed. Since then a number of additional stations were added to the network and many of the vertical component stations were replaced with three-component sensors (Fig. 1).

Events identified by the MVO are generally classified as one of several types: volcano-tectonic (VT) earthquakes, long-period (LP) events, hybrid events, or rockfalls (Miller et al., 1998). For this study we consider only VT events which are interpreted as normal double-couple earthquakes caused by rock fracture in the country rock, often in response to stress changes from intrusion of magma. Since shear-wave splitting uses particle motion analysis we only consider located events recorded on three-component instruments. Fig. 2 shows a cumulative plot of located VT events until the end of the third phase. It should be noted that VT events were recorded during the first phase of the eruption, however since many of the instruments were destroyed in 1997 there were too few stations in operation at the time to provide accurate locations, so they are not shown here. It is clear that there have been large fluctuations in the rate of VT events over the course of the study period, with increases in activity immediately preceding extrusive phases followed by a drop in the rate as the extrusion proceeds.

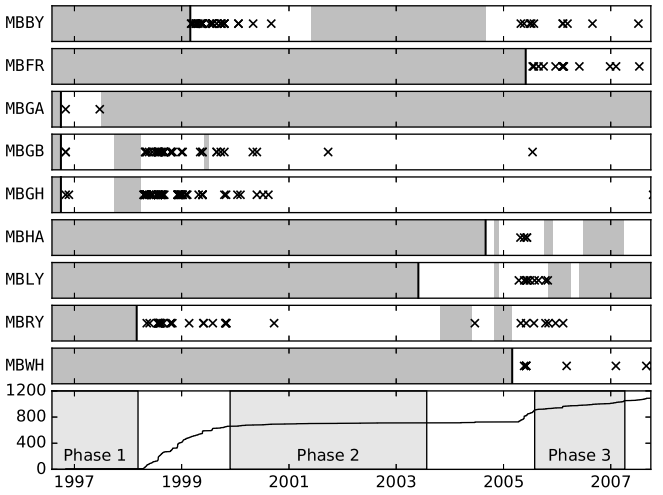

Fig. 2. Good quality splitting measurements at each station over time. Vertical black lines indicate station installation dates, with dark grey shading indicating periods when the station was not working for at least a month (Luckett, 2009). Bottom panel shows cumulative number of located VT events recorded by the network over the study period. Note that there is a data gap during the first eruptive phase since many of the instruments were not working. Large fluctuations in the rate of VT events over the course of the study period as well as changes in the seismic network configuration make temporal variations in anisotropy difficult to assess. Grey shading indicates extrusive phases of the eruption sequence.

3. Methods

The dataset for our analysis includes all located events that were classified as VT by the MVO between the years of 1996 and 2007. We repicked P- and S-arrivals for the full dataset, and only events with clear S-arrivals were used in the SWS analysis. Most of these events were approximately 2.5–4 km below sea level and thus only sample the anisotropy of the upper crust. The data were processed using the automated splitting approach of Wuestefeld et al. (2010). This method allows for the quick processing of large datasets and provides an objective quality control in the form of a quality index that ranges from −1 for null measurements (i.e. no detected SWS) to 0 for poor and +1 for good quality measurements. The quality index is based on differences in estimated splitting parameters obtained using both cross-correlation and eigenvalue methods. The ideal good measurement is characterized by identical splitting parameters from both methods (see Wuestefeld et al., 2010, for further details). The method also uses the multi-window cluster analysis of Teanby et al. (2004b) to compute clusters of measurements over different time windows and selects the results with the lowest error measurement from the lowest variance cluster. Uncertainties in ϕ and δt are calculated by finding the 95% confidence interval for the optimum values and conducting an F test on the chosen time interval (Silver and Chan, 1991).

The three component waveforms were band-pass filtered between 1 and 6 Hz prior to the splitting analysis. The choice of filter was empirically derived by trying a range of pass bands. Although VT events have energy content extending beyond 6 Hz, it was found that 1–6 Hz provided a more stable result with less scatter than with higher passbands. 'Good' measurements were selected as those with a quality index greater than 0.75, an error in fast direction of less than 20°, an error in delay time of less than 0.05 s. Measurements satisfying these criteria were further examined by eye to ensure they were of sufficient quality.

To ensure that shear wave splitting measurements are free from interference from converted phases at the surface, only arrivals with an angle of incidence less than 35° from vertical should be considered (Booth and Crampin, 1985). However, imposing a strict shear wave window of 35° based on straight line ray paths will eliminate more results than is necessary, since low velocity surface layers will result in near vertical arrivals for many events outside this window (e.g. Peacock et al., 1988). The velocity model developed for Montserrat by Paulatto et al. (2012) shows a strong vertical velocity gradient in the near surface such that we can set an effective shear wave window of 40° for events between 0 and 1.5 km below sea level, 50° for events from 1.5–3.0 km and 60° for events deeper than 3 km.

A number of the seismic stations were found to be misoriented over the period of our study. We accounted for this by using polarizations of teleseismic arrivals to correct for the station misorientations. Station MBLY was also found to have reversed polarities

Table 1
Mean value and 95% confidence interval for fast orientation $\bar{\phi}$ and delay time $\bar{\delta t}$ for each station. The $\bar{R}$ value is a measure of dispersion for circular datasets. If it is above the critical value $\bar{R}_{crit}$, which is a function of the number of measurements (n), then a preferential orientation following a von Mises distribution is present (Davis and Sampson, 2002). Fast directions passing this test are shown in bold.

Station	n	$\bar{\phi}$ (°)	$\bar{R}$	$\bar{R}_{crit(95\%)}$	$\bar{\delta t}$ (s)
MBBY	42	**−47.8 ± 8.7**	0.601	0.266	0.26 ± 0.03
MBFR	13	81.8 ± 20.8	0.411	0.475	0.27 ± 0.03
MBGA	2	48.5 ± 31.4	0.731	–	0.22 ± 0.09
MBGB	36	**58.7 ± 10.9**	0.508	0.287	0.16 ± 0.03
MBGH	66	**56.4 ± 7.9**	0.518	0.213	0.22 ± 0.01
MBHA	4	55.6 ± 35.6	0.448	0.837	0.18 ± 0.04
MBLY	10	**−39.5 ± 16.5**	0.650	0.540	0.13 ± 0.05
MBRY	33	**22.2 ± 13.2**	0.404	0.300	0.23 ± 0.03
MBWH	8	**73.2 ± 12.6**	0.818	0.602	0.28 ± 0.03

for all three components, which has been accounted for. Station MBLG was found to have a problem with the relative amplitudes of the horizontal components, so this station was omitted from further analysis. A summary of the corrections made is given in Appendix A.

4. Results and interpretation

SWS analysis resulted in 214 measurements exceeding the quality criteria across the seismic network. A statistical analysis of the measurements for each station is summarized in Table 1 and a map of rose diagrams of ϕ for each station with five or more measurements is shown in Fig. 3a. Six stations, MBBY, MBGB, MBGH, MBLY, MBRY and MBWH, show statistically significant preferred trends in ϕ. A notable characteristic is that both MBBY and MBLY show a dominant NW–SE trend in ϕ, which strongly contrasts with the NE–SW trend observed at stations MBGH and MBGB, despite their close proximity.

The spatial variation in ϕ in the southern part of the island may be related to elements of the tectonic structure (Fig. 3b). The faults of southern Montserrat represent a right step in an *en echelon* transtensional array of faults accommodating the trench parallel component of oblique convergence between the North American and Caribbean plates (Fig. 1) (López et al., 2006; Feuillet et al., 2010; Kenedi et al., 2010). Transtensional tectonic zones commonly exhibit complex strain partitioning producing local domains where stress and strain conditions may differ from surrounding regions (e.g. Dewey, 2002; Taylor et al., 2008). For example, the normal and strike slip components of displacement may be accommodated by different faults, introducing local rotations in the stress field and orientations of structures. Many of the stations surrounding SHV have a ϕ orientation similar to the WNW strike of the faults: MBBY and MBLY with a NW orientation and MBFR with a roughly E–W orientation. This suggests that the anisotropy is structurally controlled and is consistent with extension across the main structures. Stations MBGH and MBGB located to the NW of SHV are located between two of the prominent faults, the Belham Valley and Richmond Hill faults, but have NE oriented ϕ strongly oblique to strike. However, since these faults are accommodating both extension and left-lateral strike slip displacement it is possible that the region between the faults has a locally rotated extensional stress regime as illustrated in Fig. 3b. Station MBWH located north of the major structural features of the south of the island shows an E–W oriented ϕ similar to the background S_H orientation.

Seismic velocity of the shallow crust in Montserrat has been observed to be sensitive to major perturbations in the volcano over short time periods (Baptie, 2010), thus temporal variations in anisotropy may be expected. However, this is difficult to assess due to the significant fluctuations in the rates of VT events as well as changes to the seismic network over the course of the study period (Fig. 2). There were two periods of increased VT activity, the first spanning from the end of the phase 1 eruption in early 1998 until mid 2000, a few months after the onset of the phase 2 eruption. This period had a high rate of VT activity, however the

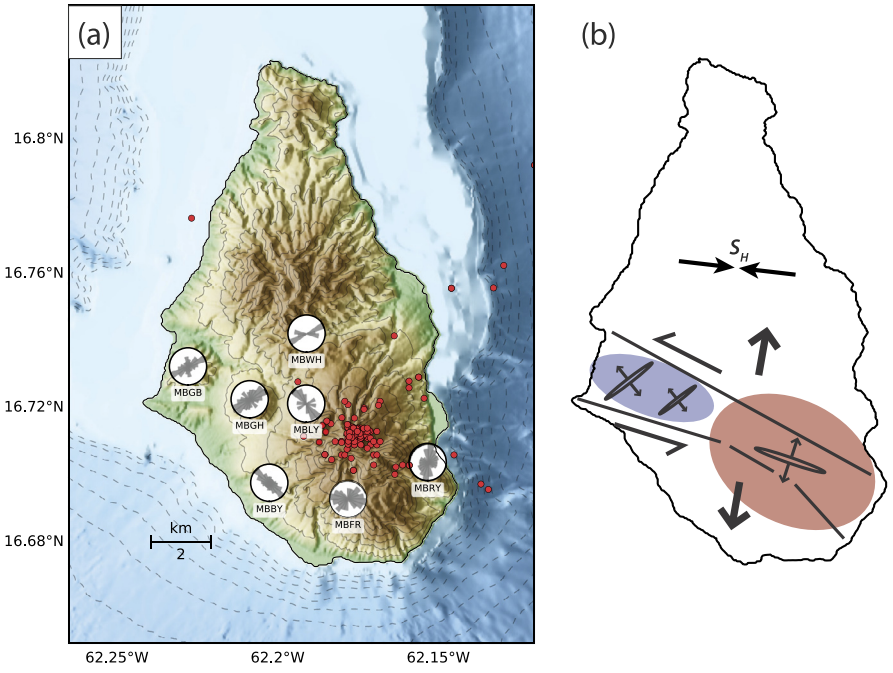

Fig. 3. (a) Map showing rose diagrams of ϕ centered at each station over the full study period. Rose diagrams are drawn such that the area of each bar is proportional to the number of measurements. Stations with statistically significant trends are drawn with a bold outline. (b) Conceptual model explaining the observed spatial variation of ϕ. Several stations show an E–W to NW–SE trend which correlates with the assumed orientation of S_H and the general trend of normal faults crossing the island (red shaded zone). Stations MBGH and MBGB show a NE–SW trend in ϕ which may be explained due to their presence between faults which are accommodating both extension and left lateral slip resulting in a localized stress rotation (blue shaded zone). (For interpretation of the references to color in this figure legend, the reader is referred to the web version of this article.)

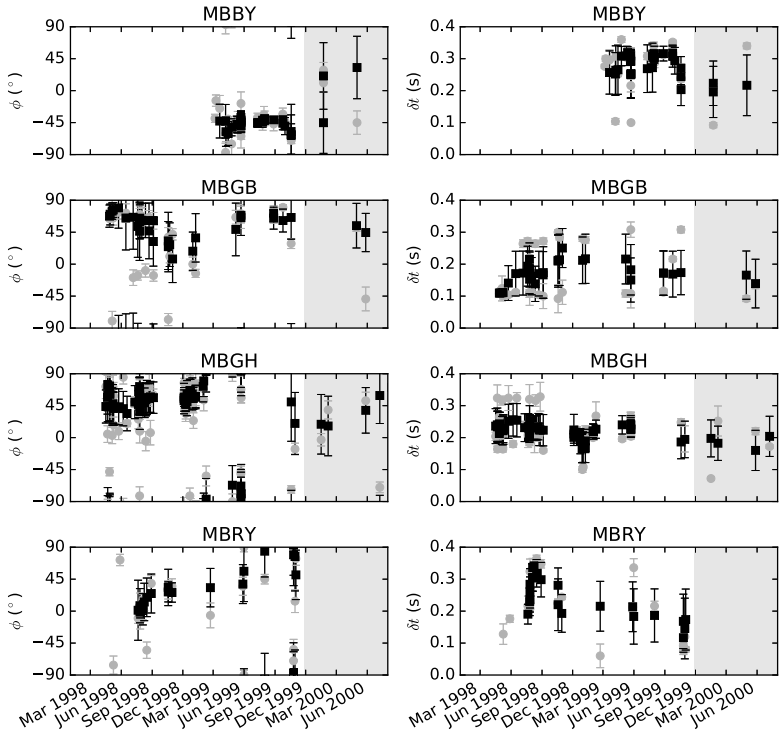

Fig. 4. Time series of ϕ and δt for stations with five or more measurements from the first period of VT activity. Light grey points are individual measurements with error bars indicating 95% confidence interval, black points are 5 point moving averages with error bars indicating 95% confidence interval of the mean. Grey shading indicates an extrusive phase of the eruption.

network was relatively sparse at the time. The second period of increased VT activity began a few months before the onset of the third extrusive phase and spanned until that eruption ceased. That period had a much broader spatial coverage, however the rate of VT events was much lower than that of the first period.

Fig. 4 shows a temporal variation in ϕ and δt at stations during the first period of activity. Station MBBY, which we interpret as being structurally controlled, shows a consistent NW orientation of ϕ throughout most of the period, with some scatter after the eruptive phase begins. Stations MBGB and MBGH both show some evidence of rotation in ϕ in the months prior to the phase 2 eruption. MBGH varies from NE in 1998 to roughly E–W in mid-1999 before returning to NE with significant scatter by the end of the year. This rotation is contemporaneous with reported variations in the p-axis orientation of VT events from dominantly NE to a mix of NE and NW in mid to late 1999, which was interpreted as being caused by stress changes associated with the pressurization of a dyke prior to the eruption (Roman et al., 2006, 2008). Thus the rotation in ϕ may be related to an overprinting of localized stresses associated with the dyke intrusion on the tectonically controlled stress field. This is consistent with our interpretation that the anisotropy at this station is stress sensitive. Station MBRY shows a NNE ϕ orientation in late 1998 and changes to scattered orientations with no clear trend in 1999.

The later period of increased VT activity, beginning in mid 2005, was recorded by a broader range of stations (Fig. 5). Over this period there is no clear evidence of temporal variation in SWS. However, the lack of data, due to the reduced rate of VT activity during this time, means that we cannot rule it out.

5. Discussion

5.1. Agreement with previous observations

Roman et al. (2011) previously investigated SWS in Montserrat over the same period. They, however, used regional earthquakes as sources instead of VT events and assumed that anisotropy was accrued from a shallow splitting layer beneath the island. This approach has a benefit in that the continuous nature of background regional seismicity allowed for easier analysis of temporal variations in SWS. However, with some events hundreds of kilometres away and others generated from the subducting slab deep below Montserrat means that it is hard to constrain where along the ray path SWS was accrued. Nevertheless, we observed SWS with an average δt of ∼0.2 s from VT events of approximately 3–4 km depth (Table 1), similar in magnitude to those reported from regional events (Roman et al., 2011) and from subducting slab events (Piñero-Feliciangeli and Kendall, 2008). This supports Roman et al. (2011) assertion that the bulk of the anisotropy beneath Montserrat is in the shallow crust, and that the upper mantle wedge above the subduction zone is relatively isotropic. The addition of deeper events and perhaps surface waves (e.g. Brisbourne et al., 1999) would help confirm this weak upper-mantle anisotropy.

It is difficult to directly compare spatial variations in anisotropy between our results and those of Roman et al. (2011), as they only present individual station data for the period from 1998 to 2005, omitting data from the many stations which were later added to the network (Fig. 2). We find that stations MBGB, MBGH, and MBRY show generally similar results to those of Roman et al. (2011), with dominantly NE oriented ϕ at MBGB and MBGH, and more scatter at MBRY but with an overall NNE trend. However, our results differ significantly at station MBBY where their NE trend contrasts markedly with our NW trend. This discrepancy is not understood. One possibility is that there may be back-azimuthal dependence of splitting parameters due to spatial variations in anisotropy. Since Roman et al. (2011) used regional events as sources with a wide range of back-azimuths it is possible that some ray-paths sample the locally rotated stress zone we interpret just to the north of MBBY (Fig. 3). Conversely, our results use events that are located directly beneath SHV and thus

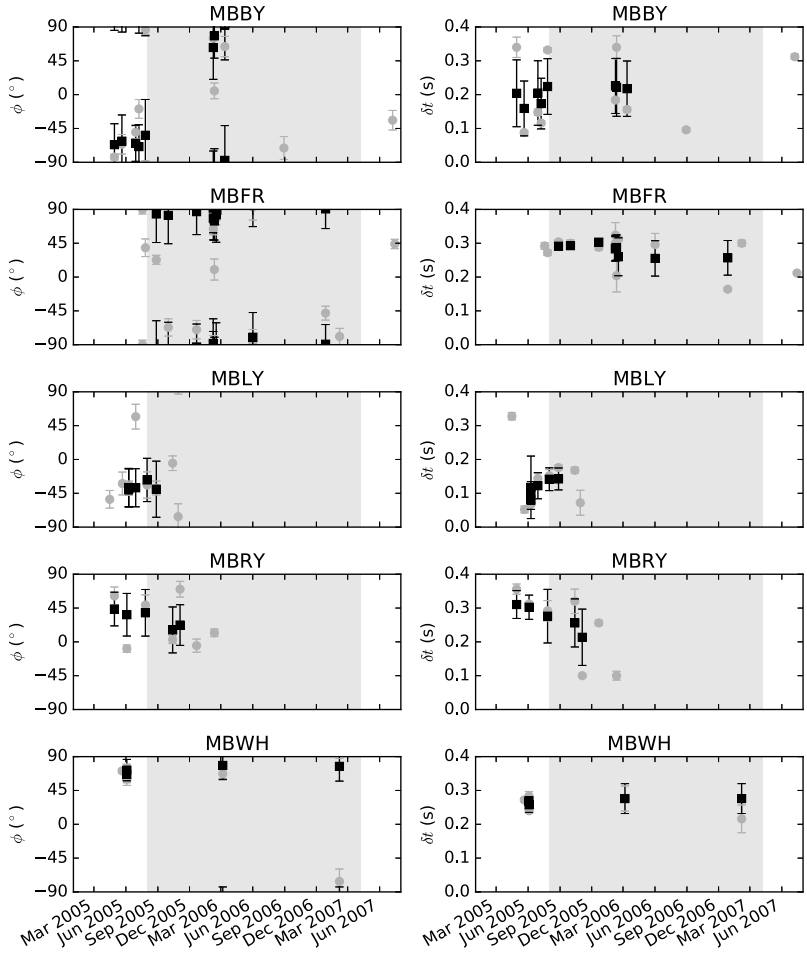

Fig. 5. Time series of ϕ and δt for stations with five or more measurements from the second period of VT activity. Light grey points are individual measurements with error bars indicating 95% confidence interval, black points are 5 point moving averages with error bars indicating 95% confidence interval of the mean. Grey shading indicates an extrusive phase of the eruption.

sample anisotropy in a relatively localized portion of the upper crust.

Roman et al. (2011) interpret their results as stress sensitive anisotropy showing local stresses associated with volcanological processes overprinting an assumed background NE oriented S_H. We disagree with this interpretation on the basis of strong geological evidence suggesting NNE extension and thus a WNW oriented S_H (e.g. Feuillet et al., 2010), as well as significant observed spatial variations in ϕ (Fig. 3). Much of the observed spatial variation is only apparent from stations deployed in 2005 beyond which Roman et al. (2011) present only aggregate rose diagrams of ϕ across the full network of stations. Nevertheless, our model does include a locally rotated NE oriented stress field affecting MBGB and MBGH. Roman et al. (2011) observe a strong (~90°) rotation of ϕ at these stations in the period of May–Nov. 1999, which they associate with stress perturbations associated with the pressurization of a dyke. We do not observe these strong rotations, but our results suggest gradual rotation in ϕ during this time, which we agree may be related to volcanological processes prior to the onset of the second eruptive phase.

5.2. Dyke orientation

One of the outstanding controversies is the orientation of the dyke feeding SHV. On the basis of recorded ground deformation, dykes with a NW to NNW orientation have been inferred for 1995–1996 (Mattioli et al., 1998), 1997 (Hautmann et al., 2009), and 2004 (Linde et al., 2010). However, Roman et al. (2006, 2008) proposed a NE trending dyke based on preferred trends in p-axes orientation of VT earthquakes that persisted over much of the same period (1996–2007). A NE oriented dyke has been inferred for 1995 based on a detailed VT earthquake analysis by Miller et al. (2010) and for 2008 based on strain measurements (Chardot et al., 2010). However, both sets of authors argue that these represent short lived trends.

Dyke orientations are typically controlled by local stress conditions, opening in the direction of minimum compression and thus aligning parallel to S_H. The interpretation of a NE oriented dyke by Roman et al. (2008) was based partially on an assumed background NE oriented S_H in the vicinity of Montserrat, which we disagree with. Our proposed model provides a mechanism to locally rotate S_H. However, we only see an indication of this to the NW of SHV and see no evidence of it occurring beneath the summit itself. Thus, the weight of evidence indicates a NNW oriented dyke is feeding SHV.

6. Conclusions

We have presented shear wave splitting analyses of VT events at Soufrière Hills volcano, Montserrat between 1996 and 2007. As these events are relatively shallow this ensures that any observed anisotropy is from the upper few kilometres of the crust. Delay times of approximately 0.2 s are similar in magnitude to previously reported SWS from much deeper events (Piñero-Feliciangeli and Kendall, 2008; Roman et al., 2011), sug-

Table A.2
Seismic station correction angles to align teleseismic polarizations with station-event back-azimuths. Positive values indicate that the horizontal components of the seismograms require a clockwise rotation. Note that station MBLY was also found to have negative polarizations of all three components. MBLG is omitted due to a scaling problem with its E component.

Time	Phase	MBBY	MBFR	MBGB	MBGH	MBLY	MBRY	MBWH
1997-05-25 23:45:29	SKS			−60°	0°			
1998-07-09 15:09:23	SKS			0°	0°		0°	
1998-12-27 01:01:57	SKS			0°	0°		0°	
1999-04-13 11:02:13	P	0°		0°	0°			
1999-08-17 00:12:09	SKS				0°		−35°	
2001-06-03 03:05:28	SKS			0°			−35°	
2001-08-02 24:03:36	SKS			0°			−35°	
2005-05-12 11:38:04	SKS	−20°		0°		10°	35°	−20°
2006-01-02 22:35:46	SKS	−20°	−40°	0°			35°	
2006-04-29 17:20:14	SKS	−20°	−40°	0°		0°	35°	−20°

gesting that anisotropy of the upper mantle wedge below Montserrat is relatively small in magnitude.

The data show substantial spatial variations in ϕ which we do not believe can be explained due to simple background stresses overprinted by local pressures associated with the volcano. Instead we find the patterns of anisotropy are strongly controlled by elements of the tectonic structure consisting of a transtensional array of faults which crosses the volcanic complex. We suggest that movement of faults across the Montserrat–Havers fault zone may support a locally rotated NE oriented S_H to the NW of SHV, relative to the ∼E–W orientation outside the zone. This stress rotation may help explain the wide variation in reported estimates of feeder dykes beneath the volcano.

Acknowledgements

We thank the sponsors of the Bristol University Microseismicity Projects (BUMPS) for funding. J.M.K. acknowledges support from the Natural Environment Research Council (grant NE/K004328/1). R.S.J.S. acknowledges support by the European Research Council (grant 228064, VOLDIES project). We are grateful to the Montserrat Volcano Observatory and the British Geological Survey for providing the data, and to Diana Roman who provided valuable information about the seismic station corrections. The manuscript benefitted greatly from the constructive reviews of Diana Roman and Geoff Wadge.

Appendix A. Station corrections

A number of seismic stations were found to be misoriented at different times during the study period. To account for this we analysed the polarizations of teleseismic arrivals (mostly SKS, but also P) compared to station-event back-azimuths to estimate a correction angle. The difficulties arising from this illustrate the importance of good field practice when deploying seismometers. The results of this analysis are summarized in Table A.2.

Station MBBY was found to be oriented correctly during the early period of VT activity, however when it was redeployed in September 2004 it was misoriented by −20°. Station MBGB was found to be misoriented by −60° prior to the destruction of the station during the first extrusive phase of the eruption, however this was corrected when the station was redeployed in April 1998. Station MBLY was found to have reversed polarizations on all three components, and to be misoriented by 10°, however this appears to have been corrected by April 2006 when the station was redeployed. Station MBRY was found to be correctly oriented early in the first high VT period, however sometime between April and August 1999 it became misoriented by −35°. We applied the correction from May 1999 onwards. During the second period of high VT activity MBRY was found to be misoriented by 35°. Station MBLG was found to have a problem with the relative amplitudes of the horizontal components and therefore was omitted from the study. Specifically the E component was found to have lower amplitudes than expected. The remaining stations were either correctly oriented or had a static correction applied for the full duration of the study.

Appendix B. Supplementary material

Supplementary material related to this article can be found online at http://dx.doi.org/10.1016/j.epsl.2015.06.006.

References

Baird, A.F., Kendall, J.-M., Verdon, J.P., Wuestefeld, A., Noble, T.E., Li, Y., Dutko, M., Fisher, Q.J., 2013. Monitoring increases in fracture connectivity during hydraulic stimulations from temporal variations in shear wave splitting polarization. Geophys. J. Int. 195 (2), 1120–1131.

Baptie, B., 2010. Lava dome collapse detected using passive seismic interferometry. Geophys. Res. Lett. 37 (19).

Boness, N., Zoback, M., 2006. Mapping stress and structurally controlled crustal shear velocity anisotropy in California. Geology 34 (10), 825–828.

Booth, D.C., Crampin, S., 1985. Shear-wave polarizations on a curved wavefront at an isotropic free surface. Geophys. J. R. Astron. Soc. 83 (1), 31–45.

Brisbourne, A., Stuart, G., Kendall, J.-M., 1999. Anisotropic structure of the Hikurangi subduction zone, New Zealand—integrated interpretation of surface-wave and body-wave observations. Geophys. J. Int. 137, 214–230.

Chardot, L., Voight, B., Foroozan, R., Sacks, S., Linde, A., Stewart, R., Hidayat, D., Clarke, A., Elsworth, D., Fournier, N., et al., 2010. Explosion dynamics from strainmeter and microbarometer observations, Soufrière Hills Volcano, Montserrat: 2008–2009. Geophys. Res. Lett. 37 (19).

Davis, J.C., Sampson, R.J., 2002. Statistics and Data Analysis in Geology, 3rd edition. Wiley, New York.

Dewey, J.F., 2002. Transtension in arcs and orogens. Int. Geol. Rev. 44 (5), 402–439.

Feuillet, N., Leclerc, F., Tapponnier, P., Beauducel, F., Boudon, G., Le Friant, A., Deplus, C., Lebrun, J.-F., Nercessian, A., Saurel, J.-M., Clément, V., 2010. Active faulting induced by slip partitioning in Montserrat and link with volcanic activity: new insights from the 2009 GWADASEIS marine cruise data. Geophys. Res. Lett. 37 (19).

Feuillet, N., Manighetti, I., Tapponnier, P., Jacques, E., 2002. Arc parallel extension and localization of volcanic complexes in Guadeloupe, Lesser Antilles. J. Geophys. Res. 107 (12).

Gerst, A., Savage, M., 2004. Seismic anisotropy beneath Ruapehu volcano: a possible eruption forecasting tool. Science 306 (5701), 1543–1547.

Hautmann, S., Gottsmann, J., Sparks, R.S.J., Costa, A., Melnik, O., Voight, B., 2009. Modelling ground deformation caused by oscillating overpressure in a dyke conduit at Soufrière Hills Volcano, Montserrat. Tectonophysics 471 (1), 87–95.

Johnson, J., Savage, M., 2012. Tracking volcanic and geothermal activity in the Tongariro Volcanic Centre, New Zealand, with shear wave splitting tomography. J. Volcanol. Geotherm. Res. 223, 1–10.

Johnson, J., Savage, M., Townend, J., 2011. Distinguishing between stress-induced and structural anisotropy at Mount Ruapehu volcano, New Zealand. J. Geophys. Res. 116 (B12), B12303.

Keats, B.S., Johnson, J.H., Savage, M.K., 2011. The Erua earthquake cluster and seismic anisotropy in the Ruapehu region, New Zealand. Geophys. Res. Lett. 38 (16).

Kenedi, C., Sparks, R., Malin, P., Voight, B., Dean, S., Minshull, T., Paulatto, M., Peirce, C., Shalev, E., 2010. Contrasts in morphology and deformation offshore Montserrat: new insights from the SEA-CALIPSO marine cruise data. Geophys. Res. Lett. 37 (19).

Le Friant, A., Harford, C., Deplus, C., Boudon, G., Sparks, R., Herd, R., Komorowski, J., 2004. Geomorphological evolution of Montserrat (West Indies): importance of flank collapse and erosional processes. J. Geol. Soc. 161 (1), 147–160.

Linde, A.T., Sacks, S., Hidayat, D., Voight, B., Clarke, A., Elsworth, D., Mattioli, G., Malin, P., Shalev, E., Sparks, S., et al., 2010. Vulcanian explosion at Soufrière Hills Volcano, Montserrat on March 2004 as revealed by strain data. Geophys. Res. Lett. 37 (19).

López, A., Stein, S., Dixon, T., Sella, G., Calais, E., Jansma, P., Weber, J., LaFemina, P., 2006. Is there a northern Lesser Antilles forearc block? Geophys. Res. Lett. 33 (7).

Luckett, R., 2009. Seismic data from the Montserrat eruption at BGS. Open Report OR/09/57. British Geological Survey.

Luckett, R., Baptie, B., Ottemoller, L., Thompson, G., 2007. Seismic monitoring of the Soufrière Hills volcano, Montserrat. Seismol. Res. Lett. 78 (2), 192–200.

Mattioli, G.S., Dixon, T.H., Farina, F., Howell, E.S., Jansma, P.E., Smith, A.L., 1998. GPS measurement of surface deformation around Soufrière Hills Volcano, Montserrat from October 1995 to July 1996. Geophys. Res. Lett. 25 (18), 3417–3420.

Miller, A., Stewart, R., White, R., Luckett, R., Baptie, B., Aspinall, W., Latchman, J., Lynch, L., Voight, B., 1998. Seismicity associated with dome growth and collapse at the Soufrière Hills Volcano, Montserrat. Geophys. Res. Lett. 25 (18), 3401–3404.

Miller, V., Voight, B., Ammon, C., Shalev, E., Thompson, G., 2010. Seismic expression of magma-induced crustal strains and localized fluid pressures during initial eruptive stages, Soufrière Hills Volcano, Montserrat. Geophys. Res. Lett. 37 (19).

Paulatto, M., Annen, C., Henstock, T.J., Kiddle, E., Minshull, T.A., Sparks, R., Voight, B., 2012. Magma chamber properties from integrated seismic tomography and thermal modeling at Montserrat. Geochem. Geophys. Geosyst. 13 (1).

Peacock, S., Crampin, S., Booth, D., Fletcher, J., 1988. Shear wave splitting in the Anza seismic gap, southern California: temporal variations as possible precursors. J. Geophys. Res. 93 (B4), 3339–3356.

Piñero-Feliciangeli, L., Kendall, J.-M., 2008. Sub-slab mantle flow parallel to the Caribbean plate boundaries: inferences from SKS splitting. Tectonophysics 462 (1), 22–34.

Roman, D., De Angelis, S., Latchman, J., White, R., 2008. Patterns of volcanotectonic seismicity and stress during the ongoing eruption of the Soufrière Hills Volcano, Montserrat (1995–2007). J. Volcanol. Geotherm. Res. 173 (3), 230–244.

Roman, D., Neuberg, J., Luckett, R., 2006. Assessing the likelihood of volcanic eruption through analysis of volcanotectonic earthquake fault-plane solutions. Earth Planet. Sci. Lett. 248 (1), 244–252.

Roman, D., Savage, M., Arnold, R., Latchman, J., De Angelis, S., 2011. Analysis and forward modeling of seismic anisotropy during the ongoing eruption of the Soufrière Hills Volcano, Montserrat, 1996–2007. J. Geophys. Res. 116 (B3), B03201.

Silver, P., Chan, W., 1991. Shear wave splitting and subcontinental mantle deformation. J. Geophys. Res. 96 (16), 16429–16454.

Taylor, T.R., Dewey, J.F., Monastero, F.C., 2008. Transtensional deformation of the brittle crust: field observations and theoretical applications in the Coso-China Lake region, eastern margin of the Sierra Nevada Microplate, southeastern California. Int. Geol. Rev. 50 (3), 218–244.

Teanby, N., Kendall, J.-M., Jones, R.-H., Barkved, O., 2004a. Stress-induced temporal variations in seismic anisotropy observed in microseismic data. Geophys. J. Int. 156 (3), 459–466.

Teanby, N.A., Kendall, J.-M., Van der Baan, M., 2004b. Automation of shear-wave splitting measurements using cluster analysis. Bull. Seismol. Soc. Am. 94 (2), 453.

Wadge, G., 1986. The dykes and structural setting of the volcanic front in the Lesser Antilles island arc. Bull. Volcanol. 48 (6), 349–372.

Wadge, G., Voight, B., Sparks, R., Cole, P., Loughlin, S., Robertson, R., 2014. An overview of the eruption of Soufrière Hills Volcano, Montserrat from 2000 to 2010. Mem. Geol. Soc. Lond. 39 (1), 1–40.

Wuestefeld, A., Al-Harrasi, O., Verdon, J.P., Wookey, J., Kendall, J.-M., 2010. A strategy for automated analysis of passive microseismic data to image seismic anisotropy and fracture characteristics. Geophys. Prospect. 58 (5), 755–773.